

# Climate change in the Hongliujing area of Lop Nur over the past 200 years revealed by the stable oxygen isotopes of *Tamarix* cones

Zhiguang LI<sup>1,2</sup>, Yaqing DONG<sup>1</sup>, Haoyu ZHANG<sup>1</sup>, Hongxiao SUN<sup>1</sup>, Danyang JIA<sup>1</sup>,  
Shikai SONG<sup>1</sup>, Yuanjie ZHAO (✉)<sup>1</sup>

<sup>1</sup> Hebei Key Laboratory of Environmental Change and Ecological Construction, College of Geographical Sciences, Hebei Normal University, Shijiazhuang 050024, China

<sup>2</sup> Hebei Center for Ecological and Environmental Geology Research, Hebei GEO University, Shijiazhuang 050031, China

© Higher Education Press 2023

**Abstract** The layers of *Tamarix* cones within sedimentary deposits in arid regions have significant chronological and paleoenvironmental implications. Here, we compare the  $\delta^{18}\text{O}$  values of *Tamarix* cones in the Hongliujing area of Lop Nur with meteorological data for the Ruoqiang meteorological station for 1960–2019 AD. Linear regression analysis was used to reconstruct the average temperature for April and the precipitation for November in the Hongliujing area over the past 200 years. The results showed that the  $\delta^{18}\text{O}$  values were significantly negatively correlated with the temperature for February, April, May, August, December, and with the annual mean temperature; significantly negatively correlated with the precipitation for February and April; significantly negatively correlated with the sunshine hours for March and May; significantly positively correlated with the sunshine hours for February, July, August, October, and December, and with the annual mean values; and significantly correlated with the relative humidity for April, July, August, September, October, and November, and with the annual mean values. Based on the  $\delta^{18}\text{O}$  record of the past 200 years, the Hongliujing area experienced two warm-wet periods (1874–1932 and 2004–2019 AD) and two cold-dry periods (1832–1873 and 1933–2003 AD). Thus, the climate was characterized by alternating warm-wet and cold-dry conditions. Wavelet analysis revealed three main cycles: 45 years, 29 years, and 14 years.

**Keywords** *Tamarix* cones, climate change,  $\delta^{18}\text{O}$ , Lop Nur

## 1 Introduction

The arid region of north-west China is climatically sensitive and vulnerable to global climate change (Zhou et al., 2019), which may profoundly affect its ecology and environment. Thus, in the context of ongoing global warming, climate change in arid north-west China has become an important scientific issue (Chen et al., 2019). Lop Nur is located within the eastern part of the Tarim Basin in Xinjiang, and it is the main endorheic lake of the Tarim Basin, where the Tarim River, Peacock River, and Cherchen River converge. Lop Nur lies within the arid zone of north-west China, and its sedimentary record preserves abundant information about the evolution of the regional climate and environment (Ma et al., 2008). Previous research on the paleoclimatic evolution of the Lop Nur area is based mainly on the sedimentary records of saline lakes (Xie et al., 2004; Jia et al., 2011; Wu and Ma, 2011; Liu et al., 2019; Li et al., 2021), and there is a lack of high-resolution paleoclimatic records. *Tamarix* (tamarisk) is distributed in patches on both banks and in the deltaic zones of the downstream reaches of the Tarim River, Hotan River, Kriya River, Cherchen River, and Peacock River, as well as in the ancient wadis and low-lying areas within the surrounding desert. Its height is generally 3–10 m, with some individuals growing to 15 m. Layers of *Tamarix* cones are intercalated with sand layers and leaf litter layers, forming a depositional sequence (Qong et al., 2002). Xia et al. (2004) discovered that the *Tamarix* cones within these deposits were a potential repository of both chronological and paleoenvironmental information. Subsequently, numerous studies of climatic and environmental change within the desert area of Xinjiang have used *Tamarix* cones as a dating tool and an environmental archive, based on

analyses of proxies such as C content, N content, sediment grain size, cation content, and stable isotopes content (Xia et al., 2005; Wang and Zhao, 2010; Wang and Zhao, 2011; Zhao et al., 2011; Liu et al., 2013; Zhang et al., 2017, 2019a; Li et al., 2019; Dong et al., 2022; Li, 2022). We studied the paleoclimatic and paleoenvironmental record of *Tamarix* cones in the western part of Lop Nur. Specifically, we measured the  $\delta^{18}\text{O}$  record of *Tamarix* cones within sedimentary deposits from the Hongliujing area in the south-eastern part of Lop Nur, and used them to reconstruct the regional climate and environment during the past 200 years.

## 2 Research region

Most of Lop Nur lies within Ruoqiang County, in Bayingol Mongolian Autonomous Prefecture, Xinjiang. It is located within the eastern part of the Tarim Basin, with the Kuruktag Mountains to the north, the Altun Mountains to the south, the Taklimakan Desert and the Kulluk Desert to the west, and the Aqik Valley to the east (Zhao et al., 2011; Zhang et al., 2021). The principal landform is desert, which contains yardangs and valleys, and has the elevation range of ~700–800 m (Zhao et al., 2011). The region has an extreme arid and warm temperate continental climate. Based on observations at Ruoqiang weather station, the average annual

precipitation is ~22 mm, the annual evaporation is as high as 3200 mm, and the relative humidity is almost zero in summer (Zhao et al., 2011). The Lop Nur region contains approximately 1% of the extant vascular plant species in Xinjiang, and is the most plant species poor area in China. It contains almost no vegetation in the salt crust, gravel desert, and Yadan areas. The vegetation in the salt desert consists of *Halocnemum* Bieb., *Halostachys* C.A. Mey, *Kalidium* Moq, *Tamarix*, and *Phragmites* Adans. The gravel desert is dotted with *Ephedra* and *Sarcogygium* Bunge. Hongliujing is located within the south-eastern part of Lop Nur, ~50 km north of Lop Nur town.

## 3 Sampling and analysis of *Tamarix* cones

### 3.1 Sampling and $\delta^{18}\text{O}$ measurements

In October 2020, a 1.76-m-thick profile of *Tamarix* cones was sampled (39.97°N, 91.01°E, Fig. 1). The section contained a well-defined alternating sequence of wind-deposited sand and leaf litter layer of *Tamarix*. After removing the surface layer, we continuously sampled the section at 2-cm intervals, which resulted in 87 samples (Fig. 2).  $\delta^{18}\text{O}$  values were measured on a stable isotope ratio mass spectrometer (EA-isolink-PLUS253, at the Institute of Botany, Chinese Academy of Sciences). The

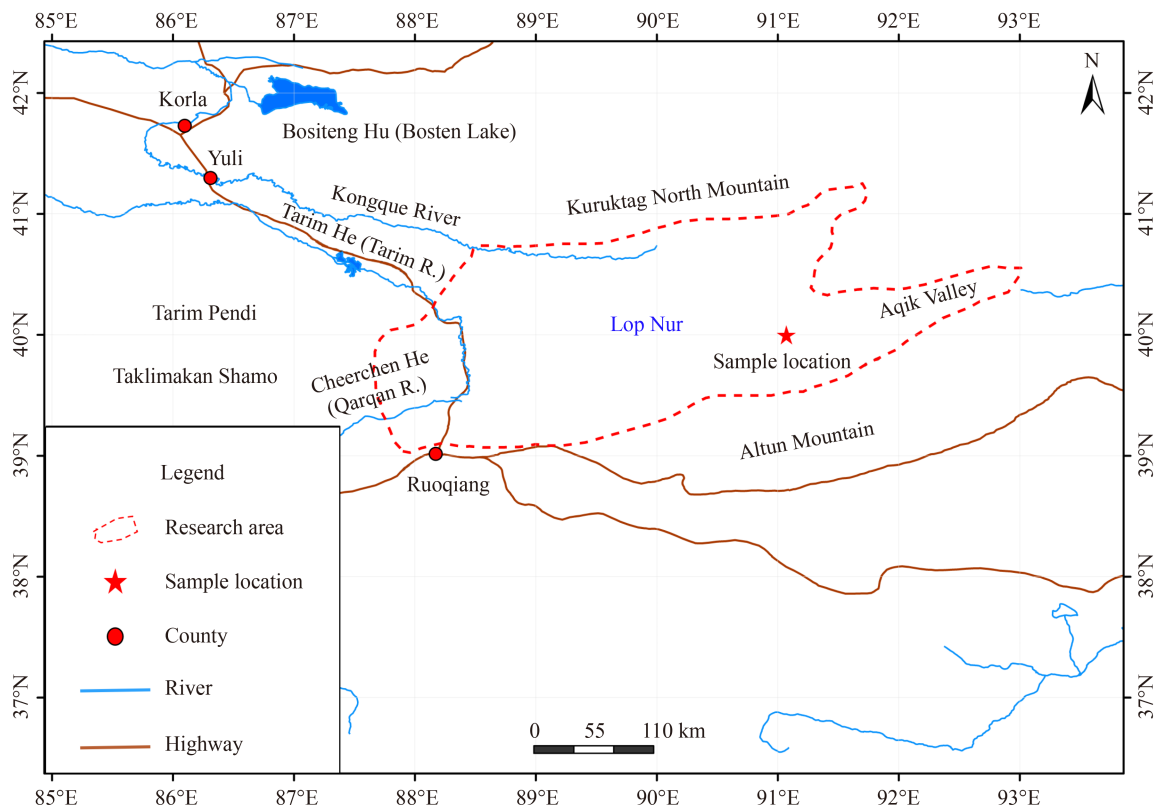


Fig. 1 Location of the sampling site in Lop Nur, north-western China.



Fig. 2 Sampling of the *Tamarix* cones.

measurements are expressed as per mil relative to Vienna Standard Mean Ocean Water (VSMOW), with the precision of  $\pm 0.3\text{‰}$ .

### 3.2 Chronology of the section

It is possible that the section has been subject to intermittent erosion by strong winds and discontinuities may be present. Based on annual layer counting, combined with the results of  $^{14}\text{C}$ ,  $^{137}\text{Cs}$ , and  $^{210}\text{Pb}$  dating in the Hongliujing area, Li (2022) established that the *Tamarix*-bearing sedimentary sequence spans the interval from 1832 to 2019 AD (Fig. 3).

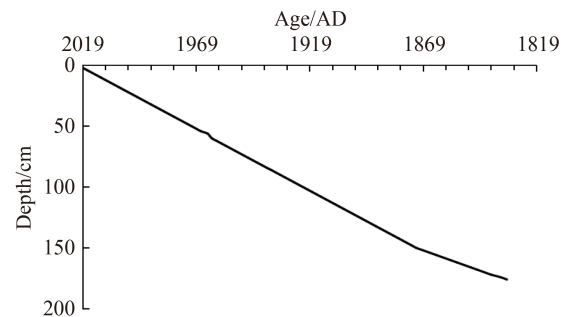


Fig. 3 The chronological sequence of the *Tamarix* cones (Li, 2022).

## 4 Oxygen isotope record of *Tamarix* cones

In the  $\delta^{18}\text{O}$  record from 1832 to 2019 AD (Fig. 4), the average  $\delta^{18}\text{O}$  value is  $29.67\text{‰}$  with the range of variation of  $14.51\text{‰}$ , and maximum and minimum values of  $38.01\text{‰}$  (in 1969 AD) and  $23.50\text{‰}$  (in 2011 AD), respectively. The  $\delta^{18}\text{O}$  values between 1954 AD and 2019 are higher (mean value of  $30.94\text{‰}$ ) than in the rest of the record, and the amplitude of fluctuations is also higher. Additionally, the maximum value of  $\delta^{18}\text{O}$  for the entire studied interval occurred during 1954–2019 AD,

while a relatively low mean value ( $29.17\text{‰}$ ) and low amplitude fluctuations ( $\sim 10.10\text{‰}$ ) occurred during 1832–1953 AD.

## 5 Relationship between $\delta^{18}\text{O}$ and climatic variables

Using meteorological data from Ruoqiang County Meteorological Station for 1960–2019 AD, we calculated Pearson correlation coefficients between  $\delta^{18}\text{O}$  and climatic variable (temperature, precipitation, sunshine hours, and relative humidity). The results are presented in Table 1.

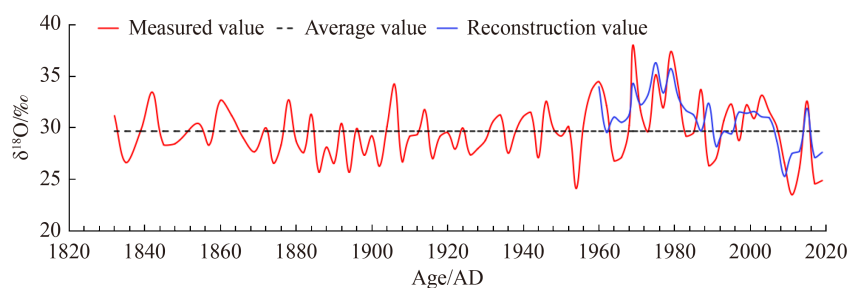


Fig. 4 The measured  $\delta^{18}\text{O}$  values and reconstruction  $\delta^{18}\text{O}$  values of *Tamarix* cones.

**Table 1** Correlation coefficients between the  $\delta^{18}\text{O}$  values of *Tamarix* cones and climatic variables

Month	Correlation coefficients			
	Mean temperature and $\delta^{18}\text{O}$	Precipitation and $\delta^{18}\text{O}$	Sunshine hours and $\delta^{18}\text{O}$	Relative humidity and $\delta^{18}\text{O}$
January	-0.267	0.218	0.001	-0.052
February	-0.374*	-0.570**	0.456*	0.207
March	-0.291	-0.211	-0.427*	0.334
April	-0.622**	0.222	-0.309	-0.382*
May	-0.570**	-0.158	-0.392*	-0.351
June	-0.249	-0.264	0.284	-0.212
July	-0.317	0.065	0.731**	-0.708**
August	-0.572**	-0.185	0.572**	-0.599**
September	0.173	-0.124	0.321	-0.621**
October	0.106	-0.082	0.456*	-0.608**
November	-0.206	-0.681**	0.160	-0.402*
December	-0.559**	0.116	0.654**	-0.302
Mean Annual	-0.535**	-0.036	0.428*	-0.439*

Notes: \* $p < 0.05$ ; \*\* $p < 0.01$ .

### 5.1 Relationship between $\delta^{18}\text{O}$ and temperature

As presented in Table 1, the relationship between the  $\delta^{18}\text{O}$  values and temperature is generally negatively correlated. It should be noted that the  $\delta^{18}\text{O}$  values have a significantly negative response to the average temperature for February, April, May, August, December, and with the annual mean temperature (correlation coefficients of  $-0.374$  ( $P < 0.05$ ),  $-0.622$  ( $P < 0.01$ ),  $-0.570$  ( $P < 0.01$ ),  $-0.572$  ( $P < 0.01$ ),  $-0.559$  ( $P < 0.01$ ), and  $-0.535$  ( $P < 0.01$ ), respectively). Additionally, the  $\delta^{18}\text{O}$  values are negatively, but not significantly, correlated with the average temperature for January, March, June, July, and November. The negative correlation between the  $\delta^{18}\text{O}$  values and temperature is consistent with previous  $\delta^{18}\text{O}$  records from Andir (Zhang et al., 2019b) and Cele (Li et al., 2019) in Xinjiang. However, there are several differences between our results and those obtained by Li et al. (2010) and Gray (1981). A positive relationship between  $\delta^{18}\text{O}$  and temperature occurs mainly in moist regions, or in moist areas within relatively arid regions. The relatively high temperatures in these areas promote transpiration, which in turn increases  $\delta^{18}\text{O}$ . In the arid Lop Nur region, the annual precipitation is 22.2 mm, and the annual evaporation is up to 3200 mm. The high temperatures of this area promote drought, which results in the closure of the stomata of *Tamarix* leaves in order to reduce transpiration.

### 5.2 Relationship between $\delta^{18}\text{O}$ and precipitation

The  $\delta^{18}\text{O}$  values have a negative response to precipitation

in most months. Specifically, the  $\delta^{18}\text{O}$  values are significantly negatively correlated with precipitation in February and November (correlation coefficients of  $-0.570$  ( $P < 0.01$ ) and  $-0.681$  ( $P < 0.01$ ), respectively). However, the correlations between  $\delta^{18}\text{O}$  and precipitation in other months are not statistically significant, which may be related to the water-use efficiency of *Tamarix* in Lop Nur. The rapid evaporation of precipitation during spring, summer, and autumn makes it difficult for precipitation to be utilized by *Tamarix*, which therefore relies mainly on groundwater for its growth. February and November are winter months in the Lop Nur area, and the relatively low evaporation during these two months promotes the persistence of snow cover, enabling moisture absorption by the branches and roots of *Tamarix*. This phenomenon is responsible for the negative correlation between  $\delta^{18}\text{O}$  and precipitation in February and November, which is consistent with research results from many other regions (Xu et al., 2015; Chen et al., 2017a).

### 5.3 Relationship between $\delta^{18}\text{O}$ and sunshine duration

The  $\delta^{18}\text{O}$  values generally have a positive response to the numbers of sunshine hours in most months. For example, the  $\delta^{18}\text{O}$  values are significantly positively correlated with the numbers of sunshine hours in February, July, August, October, December, and with the number for the whole year (correlation coefficients of 0.456 ( $P < 0.05$ ), 0.731 ( $P < 0.01$ ), 0.572 ( $P < 0.01$ ), 0.456 ( $P < 0.05$ ), 0.654 ( $P < 0.01$ ), and 0.428 ( $P < 0.05$ ), respectively). On the other hand, the  $\delta^{18}\text{O}$  values are positively, but not significantly, correlated with the numbers of sunshine hours in January, June, September, and November. However, there is a significant negative correlation between  $\delta^{18}\text{O}$  and sunshine hours in March and May (correlation coefficients of  $-0.427$  ( $P < 0.05$ ) and  $-0.392$  ( $P < 0.05$ ), respectively). The duration of transpiration, mainly during the daytime, increases with the increasing duration of sunlight, which explains the positive relationship between  $\delta^{18}\text{O}$  and the duration of sunlight. However, other studies have shown that the relationship between  $\delta^{18}\text{O}$  and sunshine hours may differ between different months (Li et al., 2019; Zhang et al., 2019a).

### 5.4 Relationship between $\delta^{18}\text{O}$ and relative humidity

There is a significant negative correlation between  $\delta^{18}\text{O}$  and the average relative humidity in April, July, August, September, October, November, and for the whole year (correlation coefficients of  $-0.382$  ( $P < 0.05$ ),  $-0.708$  ( $P < 0.01$ ),  $-0.599$  ( $P < 0.01$ ),  $-0.621$  ( $P < 0.01$ ),  $-0.608$  ( $P < 0.01$ ),  $-0.402$  ( $P < 0.05$ ), and  $-0.439$  ( $P < 0.05$ ), respectively). This may be because increasing relative humidity leads to a decrease in the numbers of leaf stomata, which reduces transpiration (Jiang, 1991; Sun

et al., 2005; Wang and Zhao, 2011; Chen et al., 2017b; Ge et al., 2018).

### 5.5 Stepwise linear regression analysis of $\delta^{18}\text{O}$ and climatic variables

We conducted a stepwise regression analysis, implemented in SPSS, in which  $\delta^{18}\text{O}$  was the dependent variable, and temperature, precipitation, sunshine hours, and relative humidity were the independent variables. The resulting regression model passed the *t*-test ( $P < 0.01$ ) (Eq. (1)):

$$Y = 33.171 - 0.246X_1 - 0.35X_2 - 2.094X_3, \quad (1)$$

where  $Y$  is  $\delta^{18}\text{O}$ ,  $X_1$  is the relative humidity in April,  $X_2$  is the relative humidity in October, and  $X_3$  is the precipitation in November. Evidently, the relative humidity in April and October, and the precipitation in November, significantly influences the  $\delta^{18}\text{O}$  values. The  $R^2$  and adjusted  $R^2$  values of this model are 0.915 and 0.896, respectively, demonstrating a satisfactory model fit to the data. The *F* test result ( $P < 0.01$ ) indicated a significant linear relationship between  $\delta^{18}\text{O}$  and the three independent variables, with the following Beta coefficients:  $-0.819$  (relative humidity in October),  $-0.542$  (precipitation in November), and  $-0.288$  (relative humidity in April). Therefore, the effect of relative humidity in October on  $\delta^{18}\text{O}$  is the most significant, followed by precipitation in November and relative humidity in April. A correlation analysis of the relationship between the  $\delta^{18}\text{O}$  of tree rings and climatic factors (temperature, precipitation, relative humidity) in Asia showed a similar trend (Chen et al., 2017a). Reference to Fig. 4 shows that the  $\delta^{18}\text{O}$  values for 1960–2019 AD obtained from this regression model agree well with the measured values.

## 6 Discussion

### 6.1 Reconstruction of the average April temperature

Among the months in which the average temperature is

significantly correlated with  $\delta^{18}\text{O}$ , the correlation coefficient for April is the strongest ( $-0.622$ ). Thus, the average temperature in April during 1832–2019 AD was reconstructed using the measured  $\delta^{18}\text{O}$  values (Fig. 5). The regression model is as follows:

$$T = -0.283\delta + 24.334, \text{ adjusted } R^2 = 0.386, P < 0.01, \quad (2)$$

where  $T$  is the average temperature in April and  $\delta$  is  $\delta^{18}\text{O}$  value.

Figure 5 shows the reconstruction results and the instrumental meteorological data for Lop Nur. The reconstructed average value of the temperature in April for 1960–2019 AD ( $15.9^\circ\text{C}$ ) is only  $0.2^\circ\text{C}$  higher than the instrumental average value ( $15.7^\circ\text{C}$ ). Thus, the reconstructed values of monthly average temperature are in good agreement with the instrumental values.

The mean of the reconstructed average temperature in April from 1832 to 2019 AD is  $16.0^\circ\text{C}$ . It should be noted that the highest ( $17.7^\circ\text{C}$ ) and lowest ( $13.6^\circ\text{C}$ ) average temperatures were in 2011 and 1969 AD, respectively, and the difference between them is  $4.1^\circ\text{C}$ .

The original average April temperatures were smoothed using a 9-year moving average (Fig. 5). The temperature in April shows an overall decreasing trend during 1832–1854 and 1895–1977 AD; however, upward trends in the average April temperature are evident during 1855–1894 and 1978–2019 AD, with the latter interval showing the more rapid rate of increase. We designate intervals with an average April temperature in most years ( $\geq 90\%$ ) larger or smaller than the average value for 1832–2019 AD as warm or cold periods, respectively. Using this convention, the temperature record of the studied interval can be divided into four periods, as listed in Table 2.

### 6.2 Reconstructed November precipitation

Among the months in which the monthly precipitation is significantly correlated with  $\delta^{18}\text{O}$ , the correlation coefficient for November is the highest (0.681). The precipitation in November during 1832–2019 AD was reconstructed using the measured  $\delta^{18}\text{O}$  values (Fig. 6). The regression model is as follows:

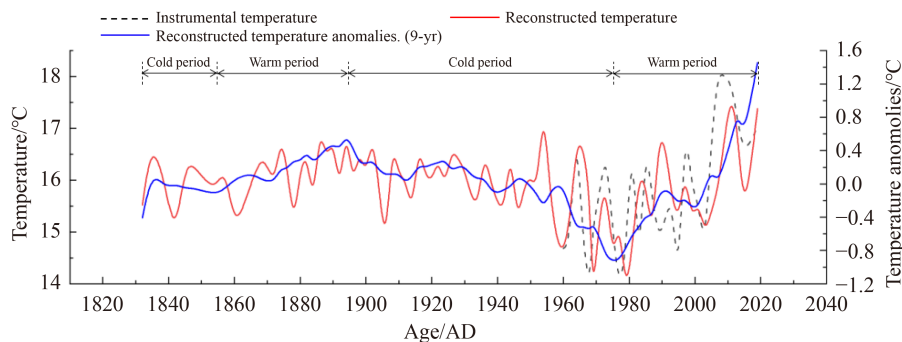


Fig. 5 Reconstructed average April temperature in Hongliujing, Lop Nur.

$$P = -0.125\delta + 4.995, \text{ adjusted } R^2 = 0.326, P < 0.01, \quad (3)$$

where  $P$  is the precipitation in November and  $\delta$  is  $\delta^{18}\text{O}$ .

Figure 6 compares the precipitation reconstruction in November and the instrumental precipitation in Lop Nur. For the precipitation in November from 1960 to 2019 AD, the reconstructed average precipitation (0.44 mm) is only 0.06 mm higher than the instrumental average value (0.38 mm). Therefore, there is good agreement between the reconstructed and instrumental precipitation.

The mean for the November precipitation from 1832 to 2019 AD is 0.51 mm. The November precipitation in 2011 AD (1.4 mm) is the highest, and there are 11 years with 0 mm of November precipitation. The raw November precipitation data were smoothed with a 9-year moving average (Fig. 6). The variation of November precipitation is essentially the same as that of the April temperature, because these two models are both based on  $\delta^{18}\text{O}$ . Similar to the definition of warm/cold periods, periods when the November precipitation for most years ( $\geq 90\%$ ) was greater than or less than the average for 1832–2019 AD were designated wet and dry periods, respectively. This enabled the precipitation record to be divided into four periods (see Table 3).

Our temperature and precipitation reconstructions

indicate that the climate of the Hongliujing area of Lop Nur during the past 200 years was characterized by two warm-wet periods (1874–1932, and 2004–2019 AD) and two cold-dry periods (1832–1873, and 1933–2003 AD).

### 6.3 Climatic comparison between different regions in northern China

The cold and warm stages reconstructed for Lop Nur are in good agreement with the two cold periods (1797–1865 and 1924–1977 AD) and one warm period (1866–1923 AD) recorded in the temperature series of the Qilian Mountains reconstructed by Wang et al. (1982), based on tree rings. Our results are also highly consistent with a tree-ring-based temperature reconstruction from June to July (smoothed with an 11-year moving average) from the central Altai Mountains obtained by Jiao et al. (2021). This record shows two warm periods (from the end of the 19th century to the 1940s, and after the mid-1990s) and one cold period (from the 1950s to the early 1990s). In addition, our results are in good agreement with one cold period (1843–1861 AD) and one warm period (1862–1964 AD) in a reconstruction of early summer temperature in the Altai Mountains obtained by Jiang et al. (2016). They are also consistent with two cold

**Table 2** Defined temperature periods in Hongliujing, Lop Nur

Temperature period	Climate	Age/AD	Duration/yr	The change of temperature/°C	Mean value/°C
Period 1	Cold	1832–1873	42	14.9–16.8	15.9
Period 2	Warm	1874–1932	59	14.1–17.1	16.2
Period 3	Cold	1933–2003	71	13.6–17.5	15.7
Period 4	Warm	2004–2019	16	15.1–17.7	16.4

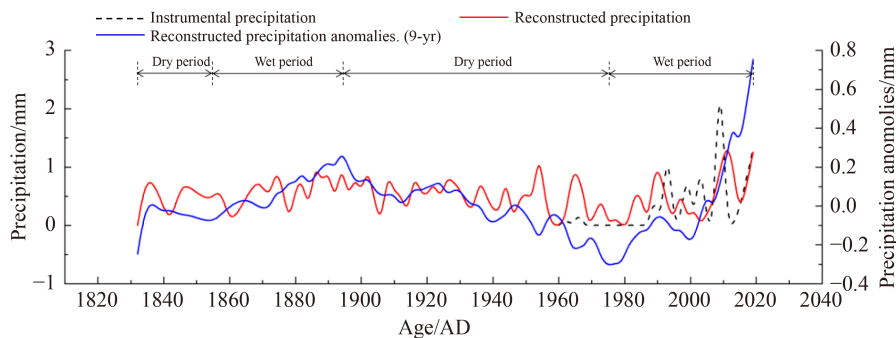


**Fig. 6** Reconstructed November precipitation in Hongliujing, Lop Nur.

**Table 3** Defined precipitation periods in Hongliujing, Lop Nur

Precipitation period	Climate	Age/AD	Duration/yr	The change of temperature/mm	Mean value/mm
Period 1	Dry	1832–1873	42	0–0.9	0.46
Period 2	Wet	1874–1932	59	0–1.1	0.62
Period 3	Dry	1933–2003	71	0–1.3	0.38
Period 4	Wet	2004–2019	16	0–1.4	0.76

periods (1832–1854 AD, 1956–2000 AD) and two warm periods (1855–1956 AD, 2000–2008 AD) in a May to August temperature series for northern Xinjiang reconstructed by Chen et al. (2017a), using tree ring density. Our temperature reconstruction is also consistent with temperature series from the Tanan region (Zhao et al., 2011; Liu et al., 2013; Zhao et al., 2016; Li et al., 2019; Zhang et al., 2019b) and Lop Nur (Sun et al., 2013), based on *Tamarix* cones; and with annual mean temperature series from the western Altay region (Zhang et al., 2008), Jinghe River Basin (Yu et al., 2007), and the Tarim River Basin (Li et al., 1988) in Xinjiang, based on tree rings. It is also consistent with the climatic record of the Guliya ice core (Zhang et al., 1999).

To assess whether the temperature reconstruction could reflect the regional scale temperature variations, the temperature series reconstructed in this paper was compared with other temperature series reconstructed from tree rings. The temperature reconstruction in northern Xinjiang (Chen et al., 2017b) (Fig. 7(a)), Mt. Altai region (Jiang et al., 2016) (Fig. 7(b)), Tibetan Plateau (Liang et al., 2008) (Fig. 7(d)), and Hongliujing area of Lop Nur (Fig. 7(e)) share a common trough in 1920s and 1970s, and then show a rapid increase after 1980s. Additionally, the temperature reconstruction in northern Xinjiang (Chen et al., 2017b) (Fig. 7(a)), Heihe River Basin (Wang et al., 2016) (Fig. 7(c)), Tibetan Plateau (Liang et al., 2008) (Fig. 7(d)), and Hongliujing

area of Lop Nur (Fig. 7(e)) peaked at the end of the 19th century.

The timing of the dry and wet periods evident in our reconstruction is in good or very good agreement with those of five other climatic reconstructions, as follows. (i) A wet period (1979–2017 AD) and a dry period (1839–1867 AD) in a tree-ring-based precipitation reconstruction for the eastern part of the Yinshan Mountains (Li et al., 2022). (ii) Four dry periods (1851–1855 AD, 1858–1868 AD, 1959–1971 AD, 1991–1996 AD) and one wet period (1889–1904 AD) in an 11-year-smoothed record of a tree-ring-based humidity index for the eastern Tianshan Mountains (Wang et al., 2007). (iii) Two dry periods (1843–1861 AD, 1974–1975 AD) and one wet period (1888–1892 AD) in a climatic reconstruction for the eastern Qilian Mountains (Hou et al., 2011). (iv) Two wet periods (1888–1904 AD, 1915–1923 AD) and four dry periods (1835–1844 AD, 1853–1887 AD, 1962–1968 AD, 1974–1985 AD) in a tree-ring-based wet/dry climatic reconstruction for eastern Xinjiang (Chen et al., 2016). (v) One dry period (1901–1990 AD) and one wet period (1991–2010 AD) in a climate reconstruction for the Tanan region based on *Tamarix* cones (Zhao et al., 2016). (vi) Two dry periods (1841–1884 AD, 1954–1986 AD) and two wet periods (1885–1899 AD, 1911–1953 AD) in a climate reconstruction for Lop Nur based on *Tamarix* cones (Sun et al., 2013). Additionally, the precipitation reconstruc-

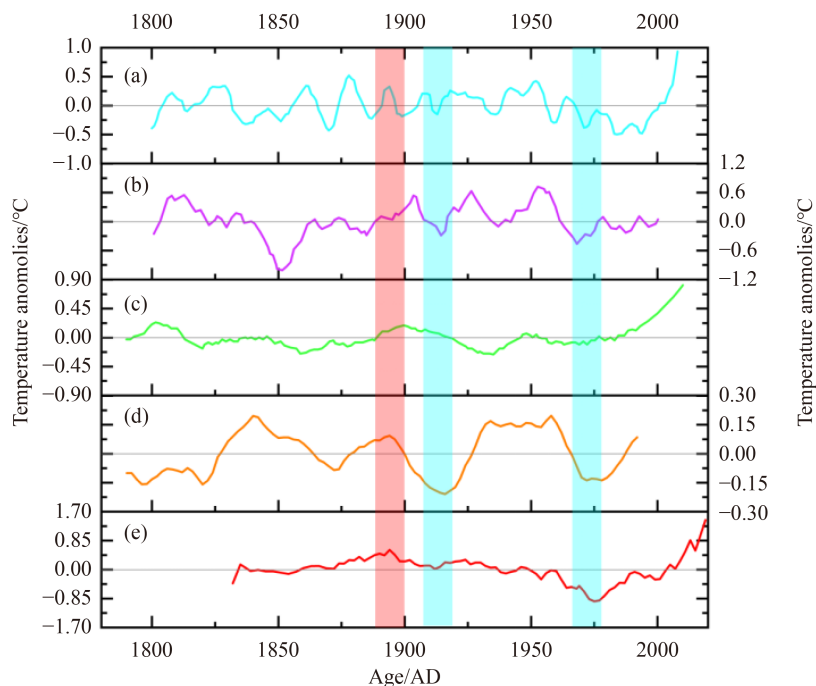


**Fig. 7** Comparison of the current study reconstructed temperature with (a) Chen et al. (2017b) tree-ring based reconstruction of temperature for the northern Xinjiang; (b) Jiang et al. (2016) tree-ring based temperature reconstruction for the Mt. Altai region; (c) Wang et al. (2016) reconstruction of temperature for Heihe River Basin using tree-ring width; (d) Liang et al. (2008) tree-ring based summer temperature reconstruction for the source region of the Yangtze River on the Tibetan Plateau; (e) reconstruction of temperature in the current study from *Tamarix* cones for Hongliujing, Lop Nur.

tions for Qinghai Lake Basin (Shi et al., 2009) and the Aksu Basin on the southern slopes of the Tianshan Mountains (Zhang et al., 2009), and the dry/wet climatic sequence for the Tanan region, based on *Tamarix* cones (Li et al., 2019; Zhang et al., 2019), are also consistent with our findings.

The precipitation series reconstructed in this study was compared with other precipitation series reconstructed based on tree rings in neighboring areas to verify the representativeness of our reconstruction on a regional scale. The precipitation reconstruction in eastern Qilian Mountains (Hou et al., 2011) (Fig. 8(b)), eastern Xinjiang (Chen et al., 2016) (Fig. 8(c)), Aksu River Basin on the southern slope of Tianshan Mountains, and Hongliujing area of Lop Nur (Fig. 8(e)) share a common trough in ~1975 AD, and peaked in ~1895 AD. In the 1920s, the precipitation in the Hongliujing area of Lop Nur (Fig. 8(e)) increased significantly, which also occurred in the Aksu River basin on the southern slope of Tianshan Mountains (Zhang et al., 2009) (Fig. 8(d)).

It should be noted that the onset and termination times of temperature and precipitation increases and decreases in our climate reconstructions are not completely synchronous with those of previous studies. Shi et al. (2002, 2003) proposed that the climate in the arid region of north-west China is “warm-wet”, which was more obvious in Xinjiang. Yao et al. (2021) produced a tree-ring-based climate reconstruction for the past 300 years

and concluded that the climate in northern Xinjiang was characterized by alternations of cold-dry and warm-wet periods. However, Zheng et al. (2020) suggested that the regional climate in Xinjiang was generally warm-dry or cold-wet.

However, the relationship between temperature and precipitation is complex, and they may not change simultaneously. Temperature and precipitation exhibit different response on different timescales. Local environmental characteristics, including fluvial runoff, lake level, vegetation cover, landforms and human activities, may result in different temperature and humidity configurations (Rehfeld and Laepple, 2016; Ljungqvist et al., 2019). Moreover, the use of different climate and environmental proxies may be an additional source of uncertainty in climate reconstructions, even within the same region.

#### 6.4 Periodicity analysis

We used Morlet wavelet analysis to characterize our climate series in the time and frequency domains. The results for precipitation were like those for temperature, and therefore we focus on the time-frequency analysis of the average temperature in April. The wavelet transform coefficients (Fig. 9(a)) indicate the presence of several cycles with a scale larger than 10 years, and that the intensity of temperature changes varied substantially over

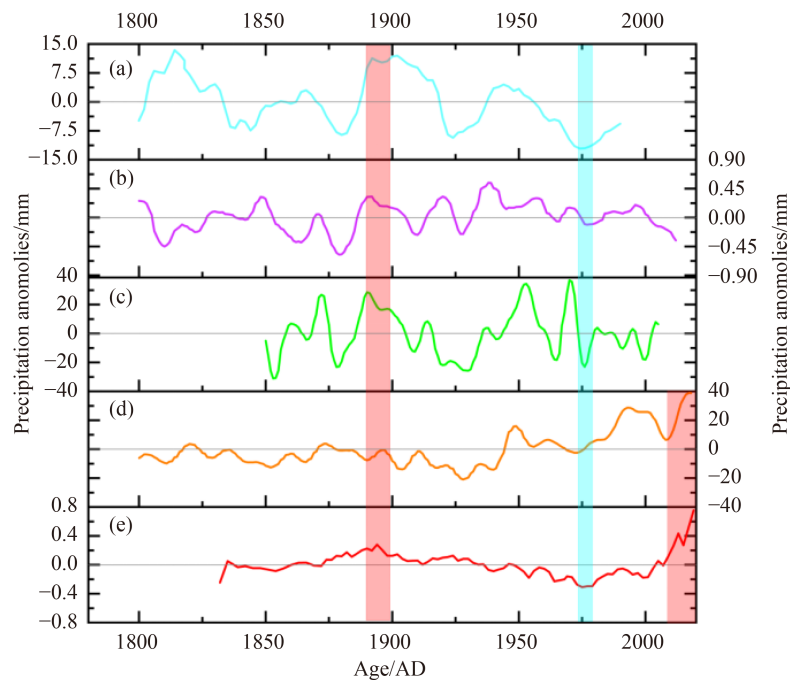


**Fig. 8** Comparison of the current study reconstructed precipitation with (a) Li et al. (2022) tree-ring based precipitation reconstruction for east of Yinshan Mountain; (b) Hou et al. (2011) reconstruction of precipitation for the eastern of Qilian Mountain using tree-ring width; (c) Chen et al. (2016) tree-ring based precipitation reconstruction for the eastern of Xinjiang; (d) Zhang et al. (2009) tree-ring based reconstruction of precipitation for Aksu River Basin on the southern slope of Tianshan Mountain; (e) reconstruction of precipitation in the current study from *Tamarix* cones for Hongliujing, Lop Nur.

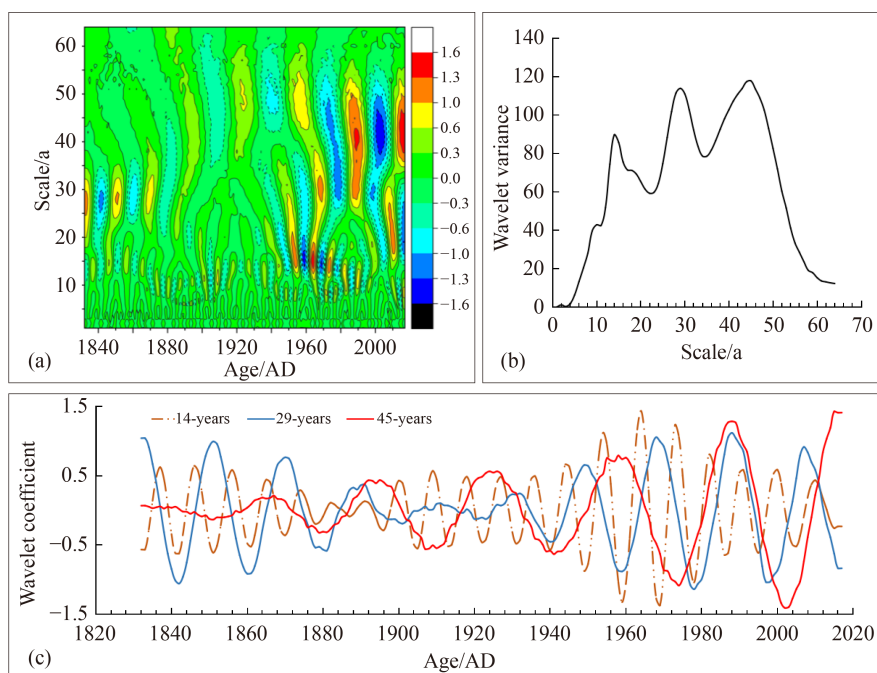


**Fig. 9** Results of wavelet analysis of the average April temperature in Hongliujing, Lop Nur. (a) Wavelet transform coefficients. (b) Wavelet variances. (c) Variation of wavelet coefficients on different timescales.

time. The wavelet variance results (Fig. 9(b)) show three distinct variance peaks with periods of 45 years, 29 years and 14 years. Analysis of the wavelet coefficients of these three main cycles (Fig. 9(c)) reveals that the corresponding mean intervals for temperature are 30.9 years, 19.5 years, and 9.2 years, respectively. No shorter cycles were evident, possibly because the sampling of *Tamarix* cones within the sedimentary sequence was not continuous, and because the reconstructed temperature and precipitation series were linearly interpolated across missing years. Although our data lack evidence of sub-9.2-year cycles, it is possible that individual 9.2-year cycles may comprise multiple 2–7-year cycles superimposed.

## 7 Conclusions

We have produced a  $\delta^{18}\text{O}$  record from layers of *Tamarix* cones intercalated within a sedimentary sequence in the Hongliujing area of Lop Nur. We used this record to analyze the relationship between  $\delta^{18}\text{O}$ , temperature and precipitation, and then to construct records of average April temperature and average November precipitation for the past 200 years. Our principal findings are as follows.

1)  $\delta^{18}\text{O}$  is significantly negatively correlated with the temperatures of February, April, May, August, and December, and with the annual mean values; significantly negatively correlated with precipitation in February and April; significantly negatively correlated with the numbers of sunshine hours in March and May;

significantly positively correlated with the numbers of sunshine hours for February, July, August, October, and December, and the annual mean values; and significantly positively correlated with relative humidity for April, July, August, September, October, and November, and with the annual mean values.

2) During the past 200 years, the Hongliujing area experienced two warm periods (1874–1932, 2004–2019 AD) and two cold periods (1832–1873, 1933–2003 AD), corresponding to two wet periods and two dry periods. Thus, the climatic configuration was characterized by the alternation of warm-wet and cold-dry intervals.

3) Three main cycles are evident in the records of average temperature in April and average precipitation in November: 45 years, 29 years, and 14 years.

**Acknowledgments** This research was supported by the National Natural Science Foundation of China (Grant No. 41877448)

## References

- Chen F, Chen J, Huang W, Chen S, Huang X, Jin L, Jia J, Zhang X, An C, Zhang J, Zhao Y, Yu Z, Zhang R, Liu J, Zhou A, Feng S (2019). Westerlies Asia and monsoonal Asia: spatiotemporal differences in climate change and possible mechanisms on decadal to sub-orbital timescales. *Earth Sci Rev*, 192: 337–354
- Chen F, Shang H, Yuan Y (2016). Comparative analysis between tree-ring based drought records of *Populus euphratica* and *Picea schrenkiana* from the mountains and plains of eastern Xinjiang. *Desert and Oasis Meteorology*, 10(01): 34–40 (in Chinese)
- Chen F, Yuan Y, Wei W, Yu S, Shang H, Zhang T, Zhang R, Wang H

- (2017b). Air temperature from May through August in northern Xinjiang reconstructed from multi-site tree-ring density. *J Glaciol Geocryol*, 39(01): 43–53 (in Chinese)
- Chen Y, Gou X H, Liu W H, Chen Q M, Su J J, Lin W (2017a). Advances in tree-ring stable oxygen isotope study in Asia. *J Glaciol Geocryol*, 39(02): 308–316 (in Chinese)
- Dong Z, Mao D, Ye M, Li S, Ma X, Liu S (2022). Fractal features of soil grain-size distribution in a typical *Tamarix* cones in the Taklimakan Desert, China. *Sci Rep*, 12(1): 16461
- Ge L, Dong X, Li L, Zhao Q, Yan D (2018). Effects of meteorological factors on daytime transpiration of Citrus Trees. *Water Saving Irrigation*, 12: 17–23 (in Chinese)
- Gray J (1981). The use of stable-isotope data in climate reconstruction. In: Wrigley T W L, Ingram M J, Farmer G, eds. *Climate and History*. Cambridge University Press: 53–81
- Hou Y, Wang N, Zhang X, Cheng H, Lu J (2011). Precipitation reconstruction from tree ring width over the eastern part of the Qilian Mountains, northwestern China. *Mountain Res*, 29(1): 12–18 (in Chinese)
- Jia H, Liu J, Qin X (2011). Early Holocene climatic changes and agricultural activities inferred from spore-pollen of Lop Nur. *J Jilin Univ (Earth Sci Ed)*, 41(S1): 181–186+194 (in Chinese)
- Jiang J (1991). Studies on resisting drought abilities of endangered species. *Arid Zone Res*, 8(2): 31–35 (in Chinese)
- Jiang S, Yuan Y, Wei W, Shang H, Zhang T, Zhang R, Qin L (2016). Early summer temperature history in the Altay Mountains recorded by tree rings during 1579–2009. *J Desert Res*, 36(04): 1126–1132 (in Chinese)
- Jiao L, Ma L, Zhang T, Wang S (2021). Changes of mean minimum temperature in June-July since 1798 in central Altay Mountain recorded by tree rings. *Acta Ecol Sin*, 41(05): 1944–1958 (in Chinese)
- Li J F, Yuan Y J, Wang C Y (1988). Temperature sequence in the area of the middle reaches of Talimu River and ITS changes in recent 200 years. *Geogr Res*, 7(03): 67–71 (in Chinese)
- Li M Q, Shao X M, Nie W Z (2022). Precipitation variation reconstructed based on tree-ring width data for the past 399 years in the eastern Yinshan Mountains, China. *Chinese J App Ecol*, 33(10): 2796–2804 (in Chinese)
- Li Q, Zhang S, Wang S, Fang Y, Li L, Zhao Y (2019). The characteristics of stable oxygen isotope in *Tamarix* cone and climatic change in recent 400 years in Qira region, Xinjiang. *Quat Sci*, 39(2): 448–457 (in Chinese)
- Li R, Xie S, Gu Y (2010). Advances in the biogeochemical study of phytolity stable isotope. *Adv Earth Sci*, 25(8): 812–819 (in Chinese)
- Li W, Mu G, Lin Y, Zhang D (2021). Abrupt climatic shift at ~4000 cal. yr B.P. and late Holocene climatic instability in arid Central Asia: evidence from Lop Nur saline lake in Xinjiang, China. *Sci Total Environ*, 784: 147202
- Li Z (2022). Research on environmental changes in Northern Lop Nur based on cations in deciduous layers of *Tamarix* Cones. Dissertation for Master's Degree. Shijiazhuang Hebei Normal University (in Chinese)
- Liang E, Shao X, Qin N (2008). Tree-ring based summer temperature reconstruction for the source region of the Yangtze River on the Tibetan Plateau. *Global Planet Change*, 61(3–4): 313–320
- Liu J, Wang R, Zhao Y, Yang Y (2019). A 40,000-year record of aridity and dust activity at Lop Nur, Tarim Basin, northwestern China. *Quat Sci Rev*, 211: 208–221
- Liu Q, Gao C, Zhao Y, Xia X (2013). Positive ion contained in *Tamarix* cone sedimentary veins and climatic and environmental change in southern region of the Taklimakan Desert. *Adv Earth Sci*, 28(12): 1326–1334 (in Chinese)
- Ljungqvist F C, Seim A, Krusic P J, González-Rouco J F, Werner J P, Cook E R, Zorita E, Luterbacher J, Xoplaki E, Destouni G, García-Bustamante E, Aguilar C A M, Seftigen K, Wang J L, Gagen M H, Esper H, Solomina O, Fleitmann D, Büntgen U (2019). European warm-season temperature and hydroclimate since 850 CE. *Environ Res Lett*, 14(8): 084015
- Ma C, Wang F, Cao Q, Xia X, Li S, Li X (2008). Climate and environment reconstruction during the Medieval Warm Period in Lop Nur of Xinjiang, China. *Sci Bull (Beijing)*, 53(19): 3016–3027
- Qong M, Takamura H, Hudaberdi M (2002). Formation and internal structure of *Tamarix* cones in the Taklimakan Desert. *J Arid Environ*, 50(1): 81–97
- Rehfeld K, Laepple T (2016). Warmer and wetter or warmer and dryer? Observed versus simulated covariability of Holocene temperature and rainfall in Asia. *Earth Planet Sci Lett*, 436: 1–9
- Shi X, Qin N, Shao X, Wang Q, Liu Y (2009). Precipitation change over the past 1000 years recorded in *Sabina tibetica* tree rings in Lake Qinghai Basin. *J Lake Sci*, 21(4): 579–586 (in Chinese)
- Shi Y, Shen Y, Hu R (2002). Preliminary study on signal, impact and foreground of climatic shift from warm-dry to warm-humid in northwest China. *J Glaciol Geocryol*, 24(03): 219–226 (in Chinese)
- Shi Y, Shen Y, Li D, Zhang G, Ding Y, Hu R, Kang E (2003). Discussion on the present climate change from Warm 2 Dry to Warm 2 Wet in northwest China. *Quatern Sci*, 23(2): 152–164 (in Chinese)
- Sun S, Huang J, Lin G, Zhao W, Han X (2005). Application of stable isotope technique in the study of plant water use. *Acta Ecol Sin*, 25(09): 2362–2371 (in Chinese)
- Sun Z, Zhang J, Zeng J, Wang H, Zhao Y (2013). The modern climate change revealed by the sedimentary veins of *Tamarix* dune in Lop Nur Region. *J Arid Land Resour Environ*, 27(07): 127–133 (in Chinese)
- Wang J, Li J, Chen F, Gou X, Peng J, Liu P, Jin L (2007). Variation of the dryness in the recent 200a derived from tree-rings width records in the east Tianshan Mountains. *J Glaciol Geocryol*, 29(02): 209–216 (in Chinese)
- Wang J, Zhao Y (2011). Reconstruction of the climate parameters in Lop Nur Region over the past 160 years based on the  $\delta D$  and  $\delta^{18}O$  in *Tamarix* cone sedimentary veins. *Quat Sci*, 31(06): 1045–1052 (in Chinese)
- Wang Y, Feng Q, Kang X (2016). Tree-ring-based reconstruction of temperature variability (1445–2011) for the upper reaches of the Heihe River Basin, Northwest China. *J Arid Land*, 8(1): 60–76
- Wang Y, Liu G, Zhang X, Li C (1982). The climatic changes recorded in the *Sabina* Genesis tree-rings in the Qilian Mountains, China and glacier fluctuations during the last 1000 years. *Chin Sci Bull*, 27(21): 1316–1319 (in Chinese)

- Wang Y, Zhao Y (2010). Pollen assemblages of *Tamarix* Cone and vegetation and climatic change in the Lop Nur Region during the past about 200 years. *Quat Sci*, 30(03): 609–619 (in Chinese)
- Wu J, Ma L (2011). Lake evolution and climatic and hydrological changes in arid zone of Xinjiang. *Marine Geol Quat Geol*, 31(2): 135–143 (in Chinese)
- Xia X, Zhao Y, Wang F, Cao Q (2005). Environmental significance exploration to *Tamarix* cone age layer in Lop Nur lake region. *Chin Sci Bull*, 50(20): 2395–2397
- Xia X, Zhao Y, Wang F, Cao Q, Mu G, Zhao J (2004). Stratification features of *Tamarix* cone and its possible significance. *Chin Sci Bull*, 49(14): 1539–1540
- Xie L, Huang S, Li F (2004). Global comparison on Palaeoclimatic change in the saline Lop Nur during the past two thousand years. *Carsol Sin*, 23(4): 311–316 (in Chinese)
- Xie L, Huang S, Li F, Zhang J (2004). Global comparison on palaeoclimatic change in the Saline Luobupo during the past two thousand years. *Carsol Sin*, (04): 55–60 (in Chinese)
- Xu G, Liu X, Chen T, An W, Wang W, Wu G, Zeng X, Wang B (2015). Climatic signals of tree-ring  $\delta^{18}\text{O}$  over the western China. *Quat Sci*, 35(5): 1218–1226 (in Chinese)
- Yao J, Mao W, Chen J, Dilinuer T (2021). Signal and impact of wet-to-dry shift over Xinjiang, China. *Acta Geogr Sin*, 76(1): 57–72
- Yu S, Yuan Y, He Q, Wu Z (2007). Reconstruction of temperature series from A.D. 1468–2001 in the Jinghe, Xinjiang. *J Glaciol Geocryol*, 29: 374–379 (in Chinese)
- Zhang R, Wei W, Yuan Y, Yu S, Yang Q (2009). A precipitation series of A.D. 1396–2005 in Aksu River Basin on the southern slopes of Tianshan Mountains: reconstruction and analysis. *J Glaciol Geocryol*, 31(1): 27–33 (in Chinese)
- Zhang S, Wang S, Li Q, Li L, Fang Y, Zhao Y (2019a). The characteristics of stable oxygen isotope in *Tamarix* cone and climate change in recent 200 years in Andier, Xinjiang. *J Arid Land Resour Environ*, 33(6): 119–125 (in Chinese)
- Zhang T, Yuan Y, Yu S, Wei W, Yang Q, Shang H (2008). Development of two tree-ring width chronologies of the samples collected from the Baluntai region. *Arid Zone Res*, 25(2): 288–294 (in Chinese)
- Zhang X, Yao T, Shi W, Li Z (1999). Record of climate change since Little Ice Age in the ice core of the Guliya Ice Cap. *J Nat Sci Hunan Normal Univ*, 22(1): 81–85 (in Chinese)
- Zhang Y, Ma L, Wang K (2021). Genesis of the Dawadi potassium nitrate deposit in Lop Nur, China. *Sci Rep*, 11(1): 22077
- Zhang Z, Fang Y, Li L, Sun Z, Zhao Y, Xia X, Ashraf M (2017). Reconstruction of the paleotemperature in the southern margin of the Taklimakan Desert based on carbon isotope discrimination of *Tamarix* leaves. *Appl Ecol Environ Res*, 15(4): 561–570
- Zhang Z, Ullah I, Wang Z, Ma P, Zhao Y, Xia X, Li Y (2019b). Reconstruction of temperature for the past 400 years in the southern margin of the Taklimakan Desert based on carbon isotope fractionation of *Tamarix* leaves. *Appl Ecol Environ Res*, 17(1): 271–284
- Zhao Y, Che G, Liu H, Zeng J, Xia X (2016). C and N content in organic matter of *Tamarix* cone and climatic and environmental change in southern region of Taklimakan desert. *Arid Land Geography*, 39(3): 461–467 (in Chinese)
- Zhao Y, Li X, Xia X, Wang X (2011). C and N contents in organic matter of *Tamarix* dune sedimentary veins and environmental change in Lop Nur Region. *J Arid Land Resour Environ*, 25(4): 149–154 (in Chinese)
- Zheng J, Zhang X, Liu Y, Hao Z (2020). The assessment on hydroclimatic changes of different regions in China at multi-scale during the past millennium. *Acta Geogr Sin*, 75(7): 1432–1450 (in Chinese)
- Zhou J, Wu J, Ma L, Qiang M (2019). Late Quaternary lake-level and climate changes in arid central Asia inferred from sediments of Ebinur Lake, Xinjiang, northwestern China. *Quat Res*, 92(2): 416–429